

Shadow of regularized compact objects without a photon sphere

Ashok B. Joshi,^{1,2,*} Vishva Patel,^{1,2,†} and Parth C. Varasani^{2,‡}

¹*PDPIAS, Charotar University of Science and Technology, Anand- 388421 (Guj), India.*

²*International Centre for Space and Cosmology, School of Arts and Sciences, Ahmedabad University, Ahmedabad-380009 (Guj), India.*

(Dated: December 23, 2025)

Recent observations by the Event Horizon Telescope (EHT) indicate that the shadow of the compact object at our Galaxy's center (Sgr A*) closely resembles that of a Schwarzschild black hole. However, identifying the presence and exact location of a photon sphere observationally remains challenging. Motivated by this, we investigate shadow formation in spacetimes that lack a photon sphere by applying the Simpson-Visser (SV) regularization technique (originally designed to smooth black hole singularities) to null singularity and charged null singularity metrics. Remarkably, these regularized null and charged null singularity spacetimes can produce a shadow without a photon sphere. We analyze how the SV regularization parameter influences their geometry and shadow size, and show that the regularized null and charged null singularity spacetimes can correspond either to two-way traversable wormholes or retain singularities. Our results reveal that shadows arising from these regularized 'null singularity spacetimes' closely mimic those of Schwarzschild and charged black-bounce spacetimes, despite the absence of a photon sphere. We also constrain parameters in these geometries using observational data of Sgr A* and M87.

keywords : Shadow, Regular compact objects, Light trajectories.

PACS numbers:

I. INTRODUCTION

Recent advances in observational astrophysics, most notably the Event Horizon Telescope (EHT) collaboration's imaging of the M87 galactic center [1–7], have opened a new window to analyze the nature of compact objects. The direct images suggest that the shadow size of the central supermassive object, Sgr A*, closely resembles that predicted for a Schwarzschild black hole [8–16]. The photon ring is the bright halo of light seen in black hole images, such as those from the EHT results. It is formed by photons that lensed very close to the maxima of the potential, sometimes orbiting the compact object more than one times before reaching our telescopes. However, observationally locating the precise location and properties of the photon sphere remains a challenge [17]. The EHT group has yet to directly resolve the photon sphere, which is still a theoretical feature. The photon ring, a lensed emission structure

that appears at about 2.6 times the Schwarzschild radius, has been identified through observation. Although this feature does not correspond to the photon sphere itself, it is in agreement with theoretical predictions and offers a useful observational probe of the strong-gravity regime near black holes [18–50].

From the observations, researchers are still trying to figure out the position of the first subring ($n = 1$), and the thickness of the first subring will provide information on the presence of the photon ring [51–53]. It is quite difficult to find direct results that determine the position of the photon sphere. However, the difference between the two conjugate subrings provides the convergence rate. Logarithmic and non-logarithmic falls provide information about the photon sphere [54]. Hence lensing in different spacetime structures provides the causal structure around the supermassive compact objects [55–60].

Examining the observational signatures of singularity nature and regularity in the context of the EHT collaboration's recent shadow investigation of the M87 galactic

*Electronic address: gen.rel.joshi@gmail.com

†Electronic address: vishvapatelnature@gmail.com

‡Electronic address: varasaniparth2014@gmail.com

centre is crucial [61–67]. Regarding our own galaxy, the GRAVITY and SINPHONI collaboration’s observations of the paths of “S” stars around our galactic center are providing incredibly valuable information. The behavior of timelike and null geodesics around singularities and other compact objects has been the subject of numerous recent investigations [68–77]. The first work on a shadow without a photon sphere was done by [78], in the null singularity spacetime. The generic end state of gravitational collapse gives the spacetime a null singularity [79]. The shadow cast by the Schwarzschild black hole is approximately five times larger than the shadow cast by the null singularity spacetime. Later work on shadows without a photon sphere is explored in various articles [80–82]. Investigating the shadows cast by a charged null singularity shows that shadows will not form in that spacetime [83]. Several studies investigated, accretion disk properties [84–91], photon spheres, which are also present in naked singularities, as well as the shadow properties in modified gravity [92–98], gravastars [99, 100], and wormholes [101–106].

This gives rise to a fundamental question: what would the observed geometry around a compact object be if a photon sphere were absent? Although traditional black hole spacetimes, such as Schwarzschild, Reissner-Nordström, and Kerr metrics, possess photon spheres that define their characteristic shadow. In [107, 108], given a proof that black holes at least have a one light ring (LR). Recent studies indicate that shadows may form even in spacetimes lacking such photon spheres [78]. For instance, thin matter shells or certain exotic compact objects can produce shadows due to their unique light-trapping properties. These findings suggest that the photon sphere is not an exclusive marker of shadow but may also appear around compact objects without the photon sphere, like horizonless objects, including naked singularities. Motivated by these insights, in this work we explore the nature of shadows cast by a class of regularized spacetimes that inherently lack photon spheres. We extend the Simpson-Visser (SV) regularization technique (originally designed to smooth black hole singularities) to null singularity and charged null singularity metrics.

It should be noted that the shadow is caused by the presence of the photon sphere in the Schwarzschild,

JNW, and JMN1 spacetimes [109, 110]. However, for a certain parameter, JNW and JMN1 can cast a shadow without a photon sphere, in JNW $n = 1/2$ and in JMN1 $M_0 = 2/3$. These findings highlight the fact that other compact objects in the presence of a photon sphere or thin shell of matter can also cast a shadow, demonstrating that it is not just a feature of black holes.

In this paper, we would like to investigate the shadow in a regular black hole and other regular compact objects. The regularized black hole was initially proposed by Bardeen [111] and further work has been carried out by Bardeen [112], Bergmann-Roman [113], Frolov [114], and Hayward [115]. Shadow properties in regular static and rotating regular black hole is discussed in [116–122]. Shadows in regularizing the JNW and JMN naked singularities discussed in [123–125]. In traditional regular black hole, Simpson and Visser proposed a different method in which the behavior of the compact object depends on the parameter L , i.e., depending on L , it is either a regular black hole or a traversable wormhole. Our key focus is on null singularity metric that, intriguingly, admit shadow formation despite the absence of photon sphere. By introducing a regularization parameter L , the SV approach replaces the singular center with a regular core or a traversable wormhole throat, modifying lightlike geodesics and potentially altering observational signatures. We investigate how this parameter influences the shadow size and how the resulting shadows compare with those from Schwarzschild and charged black hole spacetimes, as well as from null singularity spacetime.

In this work, we apply the regularization technique to null-singularity and charged null-singularity spacetimes that Simpson and Visser used. Black-bounce-Schwarzschild spacetime and Black-bounce-Reissner-Nordstrom geometry are asymptotically resembling to both. We demonstrate that, despite lacking a photon sphere or any thin shell of matter, this regularised spacetime cast a shadow. The regular center acts like a “quantum object” [126–132], with a zero-throat wormhole solution when it cannot be concealed by an event horizon in its own right, even in its ability to cast a shadow, much like a black hole or other compact objects. We consider spacetime with two free parameters: one is the mass (total mass within asymptotically flat spacetime), and the second is the regularisation parameter L (SV parameter).

The structure of the paper is as follows. In section (II), we discuss the black bounce Schwarzschild spacetime and black bounce Reissner-Nordstrom geometry in subsection (II A), and in subsection (II B), we discuss the regularized null singularity and charged null singularity spacetimes. In section (III), we discuss the nature of potential and nature of light trajectories when a photon sphere is absent around the black bounce Schwarzschild and black bounce Reissner-Nordstrom geometries and the modified null singularity and modified charged null singularity solutions presented here. We also discuss the comparative study of the shadow in the regular black hole and regular null singularity spacetime discussed here. In section (IV), we discuss the radially infalling thin accretion model for intensity distribution in regular spacetime. Using observational data of Sgr A* and M87, we constrain the parameters. Finally, in section (V), we discuss our results. Throughout the paper, we take $G = c = 1$.

II. SV-LIKE DEFORMATION IN BLACK HOLE AND NAKED SINGULARITY SPACETIMES

In this section, we discuss spherically symmetric, asymptotically flat, charged, and uncharged modified black hole and null singularity spacetimes. Using SV method in the spacetime, the metric can be given as,

$$ds^2 = -f(r)dt^2 + \frac{dr^2}{f(r)} + (r^2 + L^2)(d\theta^2 + \sin^2\theta d\phi^2) \quad (1)$$

where $f(r)$ is the metric component. We first discuss the basic spacetime properties of this spacetime. Here, consider the metric to be asymptotically flat, and when charge and mass vanish, it becomes the standard Morris-Thorne wormhole [133]. In a regular black hole, generally, null energy conditions are violated. Hence, here we have not focused on the energy condition, but we show that if a shadow without a photon sphere is observed, geometry could be mentioned in this paper.

A. Black-bounce and charged black-bounce spacetime

The metric component of a black-bounce spacetime is given as follows [134];

$$f(r) = 1 - \frac{2M}{\sqrt{r^2 + L^2}}. \quad (2)$$

There are three cases possible: i) For $L > 2M$, coordinate speed of light is non-zero, i.e. $|\frac{dr}{dt}| \neq 0$, so it is a two-way traversable wormhole for any value of r . ii) For $L = 2M$, and for the limit $r \rightarrow 0$ from any side, we have $|\frac{dr}{dt}| \rightarrow 0$, which shows a horizon at $r = 0$, but still there is no singularity, and it resembles the one-way wormhole with an extremal null throat. iii) For $L < 2M$, the coordinate speed of light $|\frac{dr}{dt}| = 0$ at horizon. There exists an event horizon at $r_e = \sqrt{4M^2 - L^2}$. Due to this parameter L , the singularity has been replaced by a regular spacelike hypersurface which represents “bounce”. All other curvature tensors remain finite in this SV-spacetime, although this SV-spacetime violates the energy conditions. Also, the SV solution can be obtained by introducing a source such as a coupled field of non-linear electrodynamics with a phantom scalar field.

A regularised charged Black-Hole or Black-Bounce-Reissner-Nordstrom spacetime or charged Black-bounce spacetime is given as [135],

$$f(r) = 1 - \frac{2M}{\sqrt{r^2 + L^2}} + \frac{Q^2}{r^2 + L^2}. \quad (3)$$

After regularisation, the domain of r has been expanded from $r \in [0, +\infty)$ to $r \in (-\infty, +\infty)$ and it preserves the asymptotic flatness. Here $L \rightarrow 0$ represents the standard Reissner-Nordstrom metric, and $M \rightarrow 0$ and $Q \rightarrow 0$ represent the standard Morris-Thorne wormhole. All curvature tensors and curvature scalars remain finite in the limit $r \rightarrow 0$, and violate null energy conditions. There exist horizons at $r_{\pm} = \sqrt{2M^2 - L^2 - q^2 \pm 2M\sqrt{M^2 - q^2}}$ and, event and Cauchy horizons are absent when $q \geq M$.

B. Regularised charged and non-charged null singularity spacetime

1. Regularised null singularity spacetime

As an example of using the SV method to regularise naked singularities, we study the SV-modified version of the null singularity metric. Null singularity metric is an end state result of a realistic gravitational collapse model [79]. The null singularity metric [78] is a static, spherically symmetric solution of the Einstein field equations for a specific matter field distribution, and is given by

the line element,

$$ds^2 = -\left(1 + \frac{M}{r}\right)^{-2} dt^2 + \left(1 + \frac{M}{r}\right)^2 dr^2 + r^2 d\Omega^2. \quad (4)$$

The parameter M is the ADM mass of the spacetime. The metric resembles the Schwarzschild spacetime in the first order of expansion, and in weak gravity, it behaves as Newtonian gravity. Now we apply the SV method via the replacement $r \rightarrow \sqrt{r^2 + L^2}$, without modifying the form dr in the metric, and the resulting metric components become

$$f(r) = \left(1 + \frac{M}{\sqrt{r^2 + L^2}}\right)^{-2}. \quad (5)$$

Here, L , the SV parameter, is a real positive quantity having dimensions of length. Also, it can readily be seen that the original symmetries and the asymptotic properties of the null singularity metric are preserved in the new one. We will get back the null singularity metric in the limit $L \rightarrow 0$. The coordinate speed of light $|\frac{dr}{dt}| \neq 0$ for this case. The geometry describes a regular two way traversable wormhole with a minimal radius throat L at $r = 0$. The causal structure is governed by the locations of horizons, determined by the roots of $f(r) = 0$. This condition does not yield physically valid solutions for the metric (5). Hence, the event horizon is absent in the given spacetime.

The definitive test of a geometry's regularity is the behaviour of its curvature invariants. For the metric (5), all polynomial scalar invariants are finite everywhere provided $L > 0$. The Ricci scalar is calculated as $r \rightarrow 0$, the Ricci scalar becomes,

$$R \rightarrow -\frac{2(-LM^4 + L^4(L + M) - L^2(3LM^2 + 4M^3))}{L(L + M)^4}, \quad (6)$$

which is finite. More comprehensively, the Kretschmann scalar $K = R_{\mu\nu\rho\sigma}R^{\mu\nu\rho\sigma}$ is also finite as $r \rightarrow 0$,

$$K \rightarrow \frac{4(2L^5 + M)^4 + L^2M^2(L^2 + ML)^2 + (L + M)^4}{L^4(L + M)^8} + \frac{(L + M)^4(L^2 + M(2L + M)^2)}{L^4(L + M)^8}, \quad (7)$$

explicitly demonstrating the absence of a curvature singularity at the spacetime's core. In the asymptotic limit $r \rightarrow \infty$, the spacetime is asymptotically flat.

Here, we analyse energy conditions in the Einstein field. The physical nature of the supporting matter is

best analyzed by the energy conditions. The Null Energy Condition (NEC), which states $T_{\mu\nu}k^\mu k^\nu \geq 0$ for any null vector k^μ , is the most fundamental of these. For a spherically symmetric fluid, this requires $\rho + p_r \geq 0$ and $\rho + p_t \geq 0$. Using the Einstein tensor from the [134], we find:

$$\begin{aligned} \rho + p_r &= \frac{1}{8\pi}(-T^t_t + T^r_r) \\ &= -\frac{L^2}{4\pi(L^2 + r^2)(L^2 + M^2 + 2M\sqrt{L^2 + r^2})}. \end{aligned} \quad (8)$$

This term is negative, indicating a clear violation of the NEC. This violation is not an incidental feature but a requirement that singularity resolution within classical general relativity is seems difficult without considering the presence of such "exotic" matter.

2. Regularized charged null singularity spacetime

The charged null singularity metric [83] is a static, spherically symmetric solution of the Einstein-Maxwell field equations. The line element of spacetime is given as follows:

$$f(r) = \left(1 + \frac{M}{r}\right)^{-2} + \frac{q^2}{r^2} \quad (9)$$

The parameters M and q are the ADM mass and the charge of the spacetime. In the weak field limit, this metric resembles the RN spacetime. Now we apply the SV method via the replacement $r \rightarrow \sqrt{r^2 + L^2}$, without modifying the form dr in the metric, and the resulting metric becomes,

$$f(r) = \left(1 + \frac{M}{\sqrt{r^2 + L^2}}\right)^{-2} + \frac{q^2}{(r^2 + L^2)}. \quad (10)$$

It can easily be verified that the original symmetries and asymptotic behaviour of the null singularity metric are maintained in the new metric. In the limit $L \rightarrow 0$, the charged null singularity metric is recovered. The coordinate speed of light $|\frac{dr}{dt}| \neq 0$ for this case. The geometry describes a regular, two-way traversable wormhole with a throat of minimal radius L at $r = 0$.

Now, analysing the behaviour of curvature scalars for the metric (10), by providing $L > 0$. The Ricci scalar as

$r \rightarrow 0$ is calculated to be:

$$R \rightarrow \frac{-2}{L^7(L+M)^4} \times \left(L^8(L+M) + L^3M^4q^2 + L^6(-3LM^2 - 4M^3 + Lq^2 + 4Mq^2) + L^4(-LM^4 + 6LM^2q^2 + 4M^3q^2) \right) \quad (11)$$

Which is finite, and also the Kretschmann scalar $K = R_{\mu\nu\rho\sigma}R^{\mu\nu\rho\sigma}$ remains finite as $r \rightarrow 0$, which resembles the absence of curvature singularity, and as $r \rightarrow \infty$ this recovers asymptotically flat spacetime. The causal structure is governed by the locations of horizons, determined by the roots of $f(r) = 0$. This condition yields, with no real solution existing for r , and hence no horizon.

For a specific kind of source, the metric is a solution to the Einstein field equations, $G_{\mu\nu} = 8\pi T_{\mu\nu}$. To analyse the nature of this kind of matter, one can use the energy conditions, specifically the Null Energy Condition (NEC), i.e. $T_{\mu\nu}k^\mu k^\nu \geq 0$ for any null vector k^μ . For a spherically symmetric fluid it requires $\rho + p_r \geq 0$ and $\rho + p_t \geq 0$. From this, we found that this condition does not hold, and it signifies some exotic matter present in this kind of spacetime.

III. SHADOWS IN REGULARIZED SPACETIMES

Considering null geodesics in the equatorial plane ($\theta = \pi/2$), the photon trajectory equation becomes [74]:

$$\frac{1}{b^2} = \frac{1}{h^2} \left(\frac{dr}{d\lambda} \right)^2 + V_{\text{eff}}, \quad (12)$$

where $V_{\text{eff}} = \frac{f(r)}{(r^2 + L^2)}$ is the effective potential, and $b = \frac{h}{\gamma}$ is the impact parameter, defined in terms of the conserved energy γ and angular momentum h . The null condition $k^\mu k_\mu = 0$, with k^μ as the photon's four-momentum, is used here.

The nature of the effective potential determines the circular photon orbits around the object. A local maximum V_{eff} corresponds to an unstable circular orbit; this defines the photon sphere. The conditions for such an orbit at radius r_{ph} are:

$$b_{\text{ph}} = \frac{\sqrt{r_{\text{ph}}^2 + L^2}}{\sqrt{f(r_{\text{ph}})}}, \quad V'_{\text{eff}}(r_{\text{ph}}) = 0, \quad V''_{\text{eff}}(r_{\text{ph}}) < 0.$$

Similarly, a local minima of V_{eff} corresponds to a stable circular: this defines the anti-photon sphere, r_{aph} . The conditions for a stable orbit are similar to the case of a photon sphere, but $V''_{\text{eff}}(r_{\text{aph}}) > 0$. If the effective potential has only a maximum, then b_{ph} gives the smallest impact parameter for which photons can escape. Light rays from distant sources with $b < b_{\text{ph}}$ are captured and cannot reach the observer, resulting in creating a shadow; in the observer's sky with a radius b_{ph} . The value of the impact parameter at $r \rightarrow 0$ is b_0 , is defined where $V_{\text{eff}}(0) = \frac{1}{b^2}$, which leads to:

$$b_0 = b_{\text{tp}}(0) = \frac{L^2}{\sqrt{f(0)}}. \quad (13)$$

However, in spacetimes where no photon sphere exists and where the effective potential diverges near the center, in such a case, shadows may not form in the same way. The effective potential remains finite at the origin, implies photons with energy $E \geq V_{\text{eff}}(0)$ can reach the singularity. Thus, photons with $b < b_0$ are trapped near the singularity, forming a shadow even in the absence of a photon sphere. This shadow can be interpreted as the shadow cast by singularity itself. Orbit equation is given as follows:

$$\frac{d^2u}{d\phi^2} = \frac{2L^2u\psi}{b^2} - \xi uf(u) - \frac{\psi u^2}{b^2} 2 \frac{df(u)}{du} \quad (14)$$

where, $\psi = (1 + l^2u^2)$ and $\xi = (1 + 2l^2u^2)$. To properly visualize shadows in an astrophysical context, one must compute the observed intensity from surrounding accretion matter. The position of the photon sphere in the black bounce, and for $L < 3M$, the photon sphere is present in that spacetime. For $L < 2M$, black bounce spacetime has an event horizon. In between $2M < L < 3M$, a photon sphere is present, but the event horizon is absent. Hence, in regular black bounce spacetime, without a black hole, a photon sphere can exist. The behavior of lightlike geodesics around the black bounce spacetime when the photon sphere is present is similar to the Schwarzschild spacetime, and when the photon sphere is absent, the lightlike geodesics are identical to the null singularity spacetime as given in Fig. 1(b). In Fig. 1(a), the effective potential is shown for different L values to illustrate the nature of potential change. The critical impact parameter at photon sphere is b_{ph} . b_{ph} is independent of L values. Hence, shadow size remain constant irrespective of L . Therefore, for

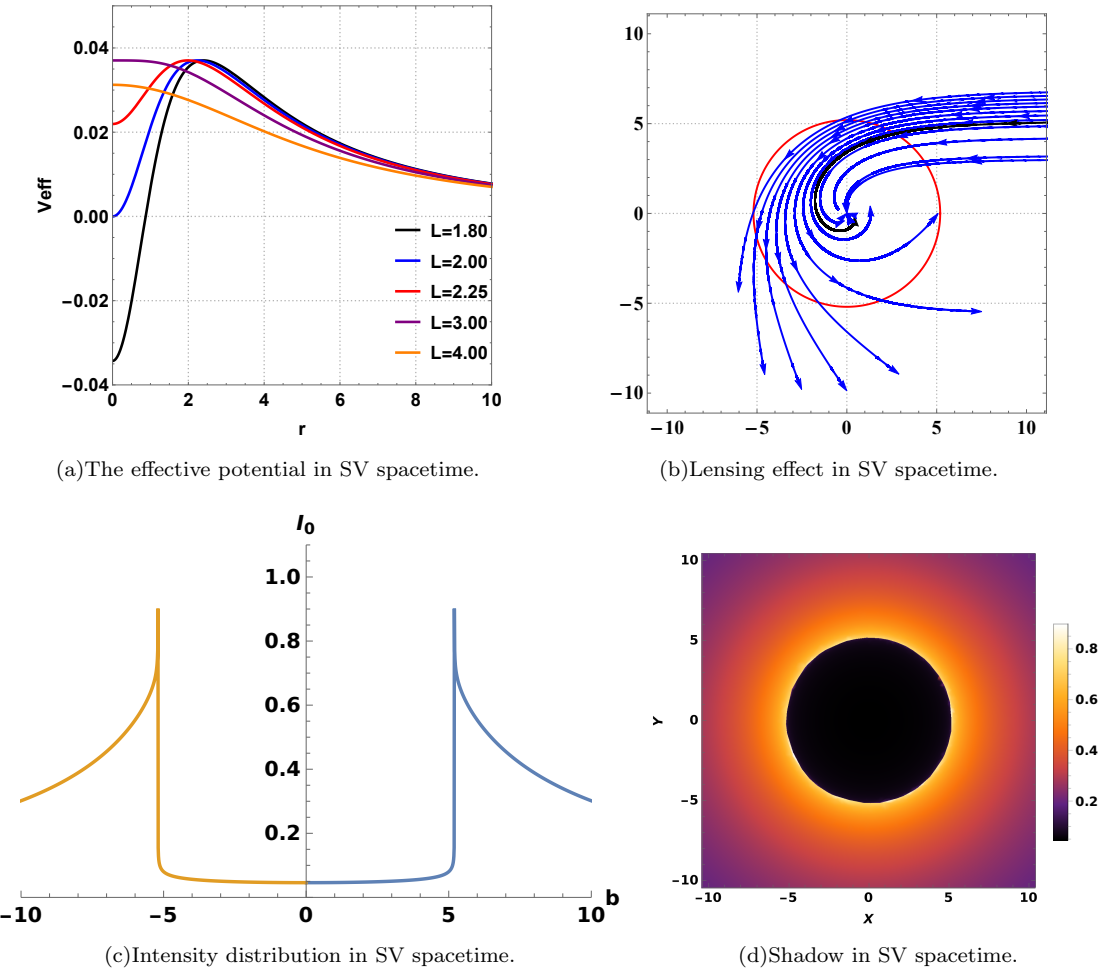


FIG. 1: In Figs. (1(a)), (1(b)), (1(c)), and (1(d)) we show the nature of effective potentials of the null geodesics, light trajectory, intensity distribution and shadow image in modified null spacetime. Effective potential of lightlike geodesics for different impact parameter in modified null spacetime is shown in Fig. (1(a)). In Fig. (1(b)) the light trajectories in these spacetimes are shown, the blue lines are the null geodesics. In Figs. (1(c)) and (1(d)), the intensity map in observer sky and the shadow of the central object are shown for modified null geometry. The shadow shown in the right bottom corner is the shadow cast by the modified null spacetime.

$L = 3M$, r_{ph} , Fig. 1(c) shows intensity distribution versus impact parameter, and Fig. 1(d) shows shadow image for distant observer.

The position of the photon sphere (r_{ph}) and antiphoton sphere (r_{aph}) are, $r_{ph} = M\sqrt{a+b}$ and $r_{aph} = M\sqrt{a-b}$, respectively, where, $a = 9/2 - x^2 - 2y^2$ and $b = (3/2)\sqrt{9 - 8y^2}$ [136]. Here, $x = L/M$ and $y = q/M$. The photon sphere and the antiphoton sphere are present in spacetime when,

$$x \leq \sqrt{\frac{9}{2} - 2y^2 + \frac{3}{2}\sqrt{9 - 8y^2}}, \quad (15)$$

and

$$x \leq \sqrt{\frac{9}{2} - 2y^2 - \frac{3}{2}\sqrt{9 - 8y^2}}, \quad (16)$$

respectively. For real values of x , the range of y , $0 < y \leq \frac{3}{2\sqrt{2}}$, which implies the $0 < x \leq \frac{9}{4}$. Therefore, within the above given range, photon sphere and anti-photon sphere are present; above that range, a shadow is always formed without a photon sphere. This range also indicates that, in the absence of an event and a Cauchy horizon, a photon sphere and an anti-photon sphere are present in the range $1 < x < \frac{3}{2\sqrt{2}}$. At $x = \frac{3}{2\sqrt{2}}$, the extremal case where, $r_{ph} = r_{aph}$. However, for certain ranges, the anti-photon sphere vanishes, but the photon

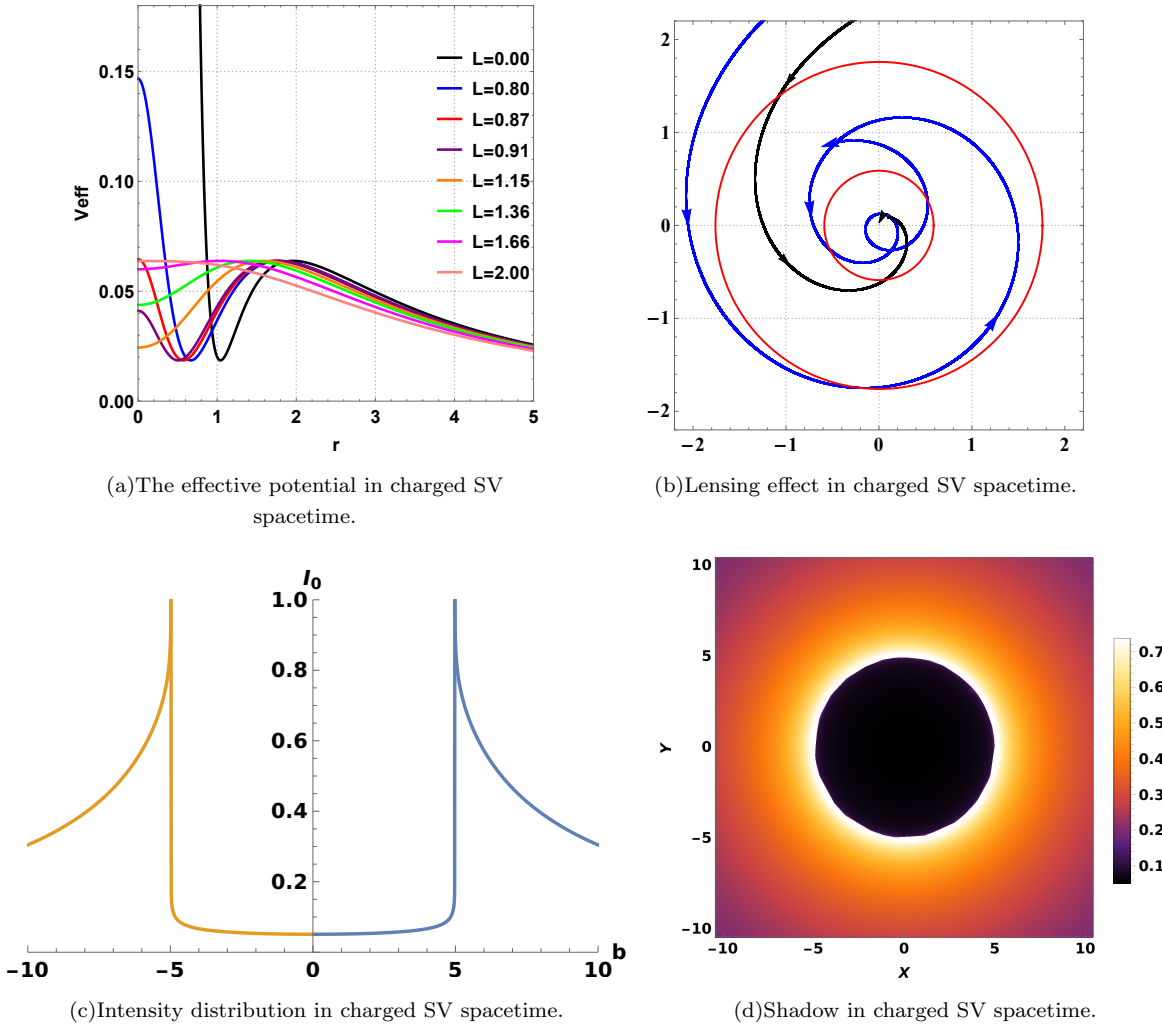


FIG. 2: In Figs. (2(a)), (2(b)), (2(c)), and (2(d)) we show the nature of effective potentials of the null geodesics, light trajectory, intensity distribution and shadow image in modified null spacetime. Effective potential of lightlike geodesics for different impact parameter in modified null spacetime is shown in Fig. (2(a)). In Fig. (2(b)) the light trajectories in these spacetimes are shown, the blue lines are the null geodesics. In Figs. (2(c)) and (2(d)), the intensity map in observer sky and the shadow of the central object are shown for modified null geometry. The shadow shown in the right bottom corner is the shadow cast by the modified null spacetime.

sphere is present in that spacetime,

$$r_{ph} = 3M \sqrt[4]{1 - \frac{8}{9}y^2}. \quad (17)$$

Hence, from Eq. (17), we can conclude that, in the absence of an antiphoton sphere, the photon sphere is always smaller than $3M$. The critical impact parameter on the photon and anti-photon spheres are,

$$b_{ph} = \frac{(\frac{9}{2} - 2y^2 + b)M}{\frac{9}{2} - y^2 + b - 2\sqrt{\frac{9}{2} - 2y^2 + b}}, \quad (18)$$

and

$$b_{ph} = \frac{(\frac{9}{2} - 2y^2 - b)M}{\frac{9}{2} - y^2 - b - 2\sqrt{\frac{9}{2} - 2y^2 - b}}, \quad (19)$$

respectively. From equations of critical impact parameter, we conclude that the size of the shadow does not change over L values. In certain cases, the local maxima of potential $V_{eff}(0) > V_{eff}(r_{ph})$, which indicates that the shadow cast by the singularity itself, instead of the photon sphere. Impact parameter values at $r = 0$ is given as follows:

$$b_0 = \frac{x^2 M}{\sqrt{x^2 - 2x + y^2}}. \quad (20)$$

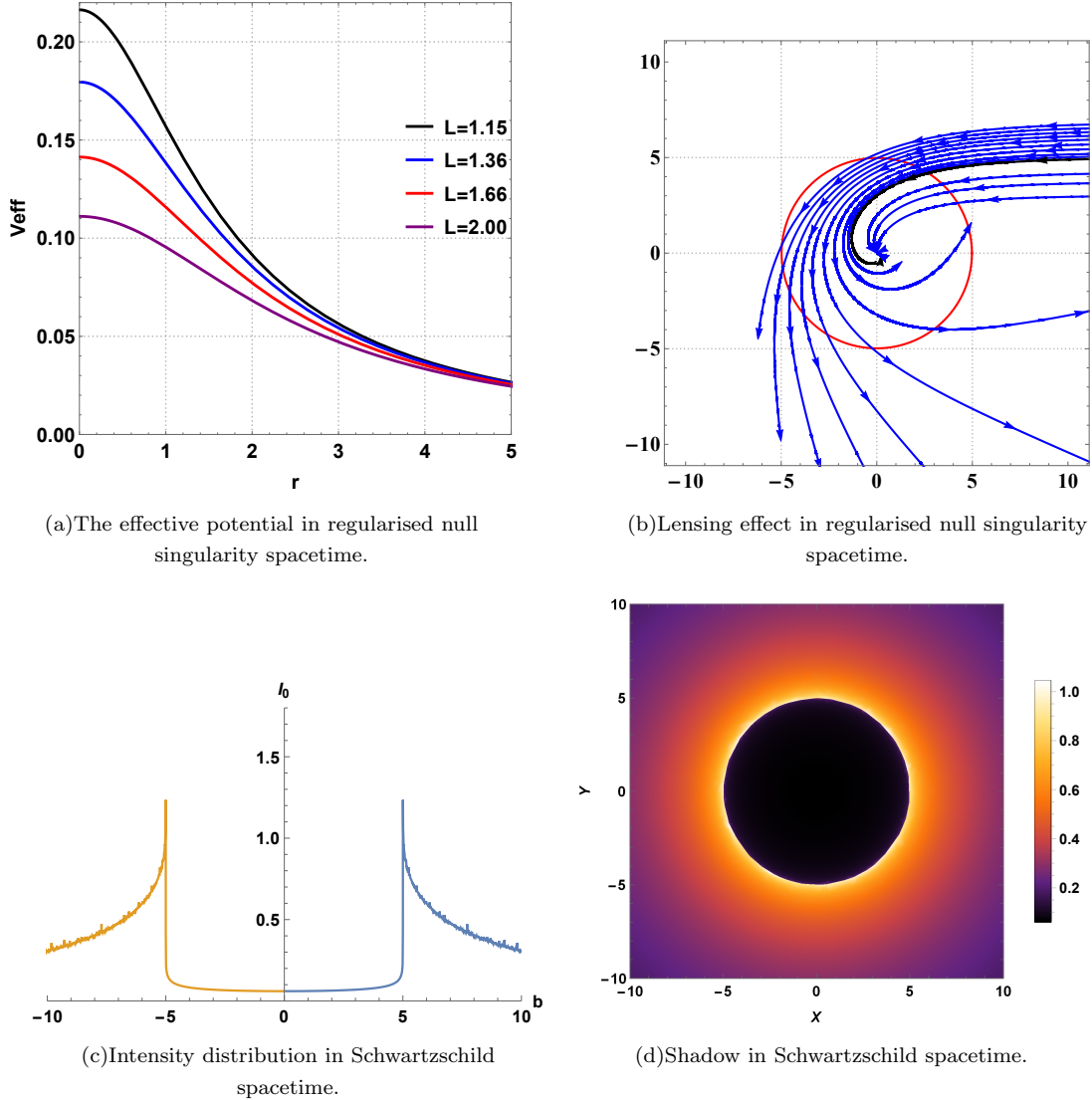


FIG. 3: In Figs. (3(a)), (3(b)), (3(c)), and (3(d)) we show the nature of effective potentials of the null geodesics, light trajectory, intensity distribution and shadow image in modified null spacetime. Effective potential of lightlike geodesics for different impact parameter in modified null spacetime is shown in Fig. (3(a)). In Fig. (3(b)) the light trajectories in these spacetimes are shown, the blue lines are the null geodesics. In Figs. (3(c)) and (3(d)), the intensity map in observer sky and the shadow of the central object are shown for modified null geometry. The shadow shown in the right bottom corner is the shadow cast by the modified null spacetime.

Here, because of the photon sphere a photon ring forms in the observer's sky. However, the size of the shadow is smaller than the photon ring formed by the photon sphere. For a critical case that is for $V_{eff}(0) = V_{eff}(r_{ph})$, $b_0 = b_{ph}$. This provides a constraint on the x that is,

$$x = \sqrt{\frac{9}{2} - 2y^2 + a}. \quad (21)$$

When $V_{eff}(0) < V_{eff}(r_{ph})$, the Photon sphere plays a crucial role in the formation of the shadow and its size. The effective potential and the behaviour of lightlike

geodesics in charged black bounce spacetime are shown in Fig. (2(a)) and Fig. (2(b)) respectively, where we take mass $M = 1$. The red circle in Fig. (1(b)), Fig. (2(b)), Fig. (3(b)) and Fig. (4(b)) shows the shadow size (b_{ph}) in given spacetime configuration. The black and blue lines show the light ray for the critical impact parameter and lensed light rays.

In a regularized null singularity spacetime, the analysis of the position of the photon sphere provides $r_{ph} = 0$. Hence, the critical impact parameter is $b_0 = (1 + x)M$.

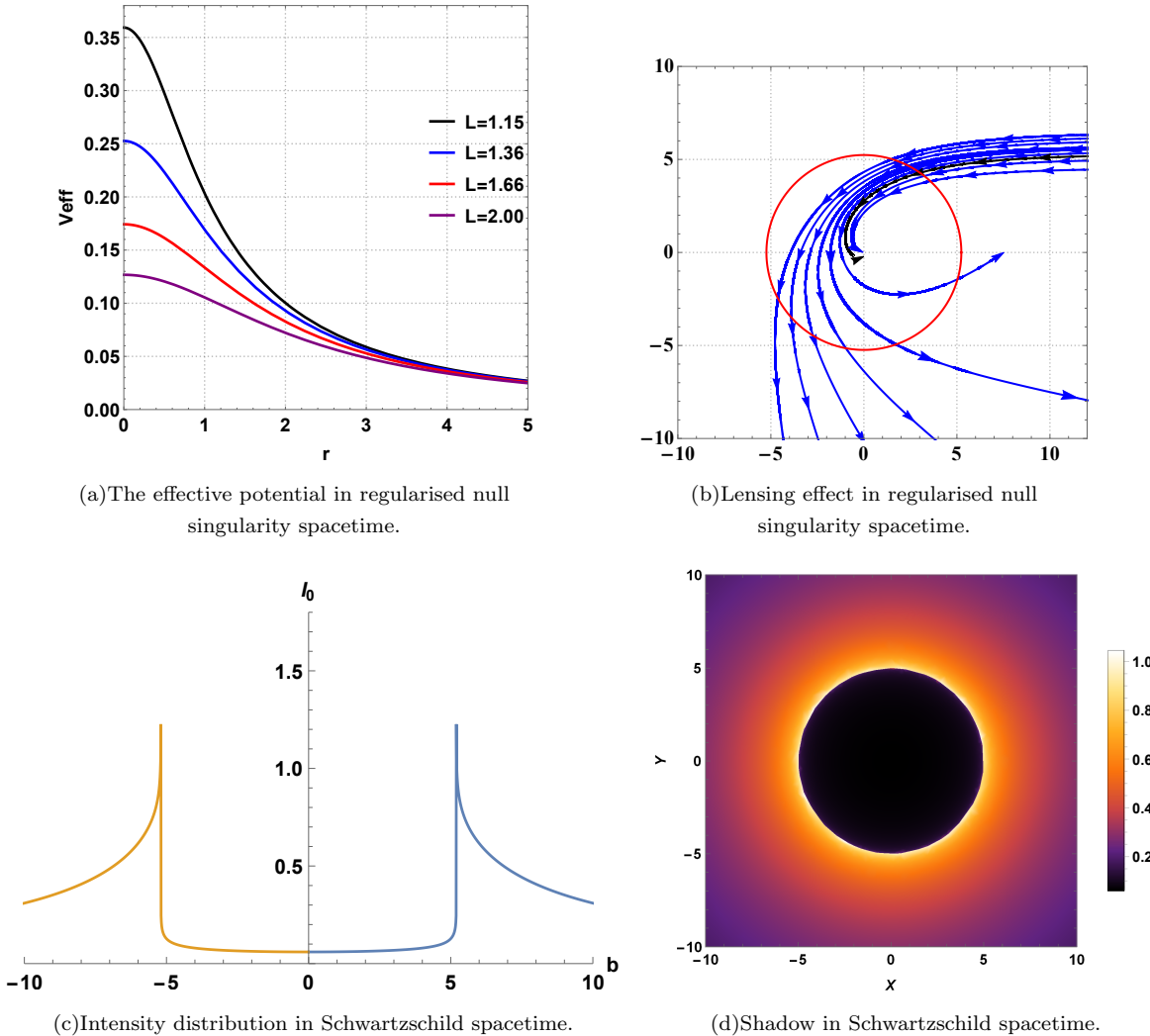


FIG. 4: In Figs. (4(a)), (4(b)), (4(c)), and (4(d)) we show the nature of effective potentials of the null geodesics, light trajectory, intensity distribution and shadow image in modified null spacetime. Effective potential of lightlike geodesics for different impact parameter in modified null spacetime is shown in Fig. (4(a)). In Fig. (4(b)) the light trajectories in these spacetimes are shown, the blue lines are the null geodesics. In Figs. (4(c)) and (4(d)), the intensity map in observer sky and the shadow of the central object are shown for modified null geometry. The shadow shown in the right bottom corner is the shadow cast by the modified null spacetime.

Therefore, the size of the shadow depends on the value of x . This provides freedom for providing observational constraints on the value of x . Fig. 3(a) shows the potential of lightlike geodesics varying with L values. For all values of L photon sphere is absent. Fig. 3(b) shows the lensing of null geodesics, which is similar to the null singularity spacetime, but the shadow size is around $3\sqrt{3}M$ as shown in intensity profile Fig. 3(c) and shadow image Fig. 3(d).

In a regularized charged null singularity spacetime, the analysis of the position of the photon sphere provides

$r_{ph} = 0$. Hence, the critical impact parameter is,

$$b_0 = \frac{x^2(1+x)M}{\sqrt{x^4 + (1+x)^2y^2}}. \quad (22)$$

Therefore, the size of the shadow depends on the value of x and y . This provides freedom for providing observational constraints on the value of x and y . Fig. 4(a) shows the potential of lightlike geodesics varying with L and q values. For all values of L and q photon sphere is absent. Fig. 4(b) shows the lensing of null geodesics, which is similar to the null singularity spacetime, but the shadow size is around $3\sqrt{3}M$ as shown in intensity profile

Fig. 4(c) and shadow image Fig. 4(d).

IV. INTENSITY DISTRIBUTIONS AROUND COMPACT OBJECTS

In this work, we assume spherically symmetric, radially infalling thin accretion matter that emits monochromatic radiation. The emissivity (in the emitter's frame) is modeled as:

$$j(\nu_e) \propto \frac{\delta(\nu_e - \nu_*)}{r^2}, \quad (23)$$

where ν_e is the photon frequency in the emitter's rest frame. The observed intensity on the distant sky, in terms of image-plane coordinates (X, Y) , is given by [101]:

$$I_{\nu_o}(X, Y) = \int_{\gamma} g^3 j(\nu_e) dl_{\text{prop}}, \quad (24)$$

with redshift factor $g = \nu_o/\nu_e$, and proper length element in the emitter's frame:

$$dl_{\text{prop}} = -k_{\alpha} u_e^{\alpha} d\lambda.$$

Here, k^{μ} is the photon's four-momentum, u_e^{μ} is the four-velocity of the emitter, and λ is the affine parameter. For a distant static observer, $u_o^{\mu} = (1, 0, 0, 0)$, the redshift factor becomes:

$$g = \frac{k_{\alpha} u_o^{\alpha}}{k_{\beta} u_e^{\beta}}. \quad (25)$$

For radial infall, the emitter's four-velocity components are:

$$u_e^t = \frac{1}{g_{tt}}, \quad u_e^r = -\sqrt{\frac{1-g_{tt}}{g_{tt}g_{rr}}}, \quad u_e^{\theta} = u_e^{\phi} = 0. \quad (26)$$

Substituting these gives the redshift factor as:

$$g = \frac{1}{\frac{1}{g_{tt}} - \frac{k_r}{k_t} \sqrt{\frac{1-g_{tt}}{g_{tt}g_{rr}}}}, \quad (27)$$

where

$$\frac{k^r}{k^t} = \sqrt{\frac{g_{tt}}{g_{rr}} \left(1 - \frac{g_{tt}b^2}{r^2 + L^2}\right)}. \quad (28)$$

The final expression for the observed intensity becomes [101]:

$$I_o(X, Y) \propto - \int_{\gamma} \frac{g^3 k_t dr}{(r^2 + L^2) k^r}, \quad (29)$$

where $X^2 + Y^2 = b^2$. Using Eq. (29), the shadow profile as seen by a distant observer can be simulated.

A. Observational constraints

When it comes to observation, the BH shadow diameter is important since high-resolution very long baseline interferometry (VLBI) observations, particularly those carried out by the EHT Collaboration, can directly restrict it. The EHT has produced unprecedented measurements of the shadow size by imaging the vicinity of supermassive compact objects like Sgr A* and M87*. Based on these observational data, we can restrict the parameters M , L , and q . These data serve as a crucial testbed for examining departures from the Kerr metric's predictions. They are among the most direct probes of the strong-gravity regime near the event horizon. The appropriate limitations on the dimensionless shadow radius rsh/M can be inferred as follows using the observed angular diameters and the mass estimates of these BHs [64, 137]:

$$\begin{aligned} \text{Sgr A}^* : & \quad \begin{cases} 1\sigma : 4.55 \lesssim \frac{r_{\text{sh}}}{M} \lesssim 5.22, \\ 2\sigma : 4.21 \lesssim \frac{r_{\text{sh}}}{M} \lesssim 5.56. \end{cases} \\ \text{M87}^* : & \quad \begin{cases} 1\sigma : 4.75 \lesssim \frac{r_{\text{sh}}}{M} \lesssim 6.25, \\ 2\sigma : 4.00 \lesssim \frac{r_{\text{sh}}}{M} \lesssim 7.00. \end{cases} \end{aligned}$$

In Fig (5), Shadow radius in the null and charged null regularized spacetime compared with the EHT observational bounds for Sgr A* and M87. Figs. 5(a) and 5(b) show the variation of the normalized shadow radius Rsh/M with respect to the parameter l/M for the neutral case, while the shaded regions represent the 1σ and 2σ observational constraints derived from the EHT measurements of Sgr A* and M87, respectively. Figs. 5(c) and 5(d) correspond to the charged null regular geometry, where the influence of the charge parameter q/M on the shadow radius is demonstrated for different values $q/M = 0, 0.5, 1.0$, and 1.5 . The shadow radius increases slightly with higher charge, indicating a deviation from the Schwarzschild limit. The colored bands denote the observational ranges within which the theoretical shadow size remains consistent with the EHT observations. Overall, the comparison shows that both Sgr A* and M87 constraints restrict the allowed parameter space of the null regular geometry, with the neutral case lying well within the observational limits and higher charges leading to marginally larger deviations.

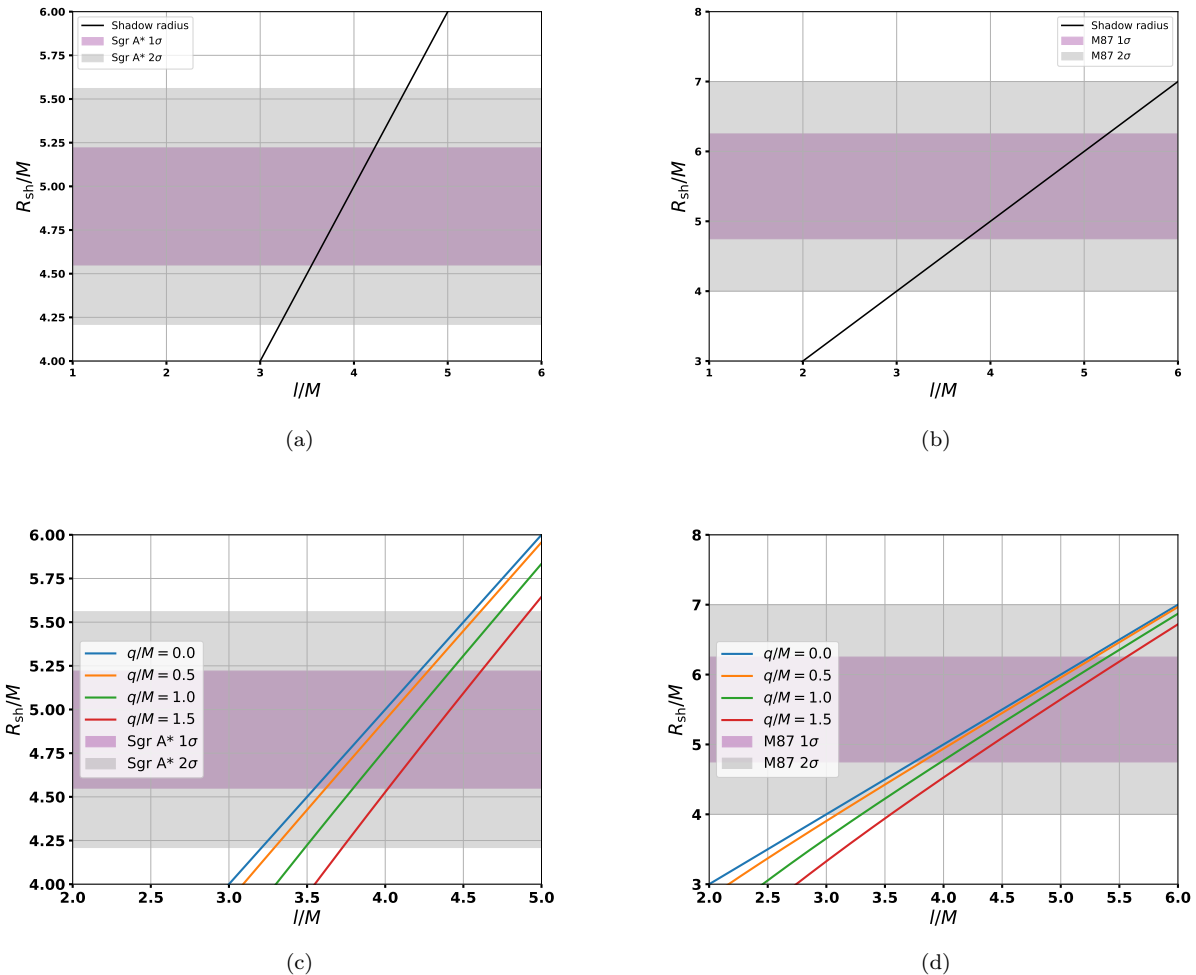


FIG. 5: Shadow radius in null regular geometry compared with Sgr A^* and M87 for 1σ and 2σ constraints derived from the EHT observations are presented in Figs. 5(a) and 5(b) respectively. Shadow radius in charged null regular geometry compared with Sgr A^* and M87 for 1σ and 2σ constraints derived from the EHT observations are presented in Figs. 5(c) and 5(d) respectively.

V. CONCLUSION

In this work, we examined the behavior of light rays and the resulting shadow structure in a class of regularized spacetimes constructed through the Simpson–Visser procedure. Since strong-gravity lensing carries crucial information about the nature of the central object, we analyzed how these geometries cast shadows despite lacking conventional photon spheres. Our results show that the presence of a bright photon ring does not necessarily imply the existence of a photon sphere, and we find situations where both a photon and an anti-photon sphere are present while the shadow is cast primarily by the gravitational center itself. In such cases, the bright photon ring is associated with the

photon sphere, but the shadow size remains smaller than the ring, indicating that the shadow originates from the regularized core rather than from any unstable light orbit.

A key outcome of our analysis is that the shadows produced by these regularized null singularity spacetimes closely resemble those of the Schwarzschild black hole, even though their causal structures differ fundamentally and no photon sphere is required to form a shadow. We further demonstrate that the location of the photon sphere, when present, does not uniquely determine the shadow size. This has significant implications for interpreting high-resolution observations of compact

objects, including Sgr A*, where distinguishing between classical black holes and alternative compact objects remains a central challenge.

Several studies suggest that the regularization parameter L may give quantum gravitational information. In this interpretation, L smooths the classical singularity by introducing effects that become dominant near the gravitational center. If such quantum corrections influence photon trajectories in the strong-field region, they may leave observable imprints on the shadow cast by the regularized core. Identifying and characterizing these properties would require a more detailed investigation of the precise features that lie within the shadow structure.

Overall, our study indicates that the shadow structures observed by the EHT collaboration could, in principle, arise even in spacetimes without event horizons or

photon spheres. Similar observational features can emerge from exotic compact configurations, including regularized null singularities. This is possibly linked to mechanisms of singularity resolution in quantum gravity. These insights broaden the range of physically viable models consistent with current observations and highlight the need for additional observational tests to uncover the true nature of supermassive objects at galactic centers.

VI. ACKNOWLEDGMENTS

VP acknowledges the support of the Council of Scientific and Industrial Research (CSIR, India; Ref: 09/1294(18267)/2024-EMR-I) for financial support.

[1] K. Akiyama *et al.* [Event Horizon Telescope], *Astrophys. J. Lett.* **875**, L1 (2019)

[2] K. Akiyama *et al.* [Event Horizon Telescope], *Astrophys. J. Lett.* **875**, no.1, L2 (2019)

[3] K. Akiyama *et al.* [Event Horizon Telescope], *Astrophys. J. Lett.* **875**, no.1, L3 (2019)

[4] K. Akiyama *et al.* [Event Horizon Telescope], *Astrophys. J. Lett.* **875**, no.1, L4 (2019)

[5] K. Akiyama *et al.* [Event Horizon Telescope], *Astrophys. J. Lett.* **875**, no.1, L5 (2019)

[6] K. Akiyama *et al.* [Event Horizon Telescope], *Astrophys. J. Lett.* **875**, no.1, L6 (2019)

[7] D. Psaltis *et al.* [Event Horizon Telescope], *Phys. Rev. Lett.* **125**, no.14, 141104 (2020).

[8] K. Akiyama *et al.* [Event Horizon Telescope], *Astrophys. J. Lett.* **930** no.2, L12 (2022).

[9] K. Akiyama *et al.* [Event Horizon Telescope], *Astrophys. J. Lett.* **930** no.2, L13 (2022).

[10] K. Akiyama *et al.* [Event Horizon Telescope], *Astrophys. J. Lett.* **930** no.2, L14 (2022).

[11] K. Akiyama *et al.* [Event Horizon Telescope], *Astrophys. J. Lett.* **930** no.2, L15 (2022).

[12] K. Akiyama *et al.* [Event Horizon Telescope], *Astrophys. J. Lett.* **930** no.2, L16 (2022).

[13] K. Akiyama *et al.* [Event Horizon Telescope], *Astrophys. J. Lett.* **930** no.2, L17 (2022).

[14] J. Farah *et al.* [Event Horizon Telescope], *Astrophys. J. Lett.* **930** no.2, L18 (2022).

[15] M. Wielgus *et al.* [Event Horizon Telescope], *Astrophys. J. Lett.* **930** no.2, L19 (2022).

[16] A. E. Broderick *et al.* [Event Horizon Telescope], *Astrophys. J. Lett.* **930** no.2, L21 (2022).

[17] A. Eichhorn, A. Held and P. V. Johannsen, *JCAP* **01**, 043 (2023).

[18] A. B. Abdikamalov, A. A. Abdujabbarov, D. Ayzenberg, D. Malafarina, C. Bambi and B. Ahmedov, *Phys. Rev. D* **100**, no. 2, 024014 (2019).

[19] A. E. Broderick and K. Salehi, *Astrophys. J.* **977**, no.2, 249 (2024).

[20] F. Atamurotov, B. Ahmedov, and A. Abdujabbarov, *Phys. Rev. D* **92**, 084005 (2015).

[21] S. Vagnozzi and L. Visinelli, *Phys. Rev. D* **100**, no. 2, 024020 (2019).

[22] G. Gyulchev, P. Nedkova, T. Vetsov and S. Yazadjiev, *Phys. Rev. D* **100**, no. 2, 024055 (2019).

[23] Ramesh Narayan, Michael D. Johnson, and Charles F. Gammie, *The Astrophysical Journal Letters*, Volume 885, Number 2.

[24] S. E. Gralla, D. E. Holz and R. M. Wald, *Phys. Rev. D* **100**, no. 2, 024018 (2019).

[25] A. A. Abdujabbarov, L. Rezzolla, and B. J. Ahmedov, *Mon. Not. R. Astron. Soc.* **454**, 2423 (2015).

[26] G. P. Li and K. J. He, *JCAP* **06**, 037 (2021).

[27] R. Kumar Walia, P. Kocherlakota, D. O. Chang and K. Salehi, *Phys. Rev. D* **111**, no.10, 104074 (2025).

[28] K. Salehi, R. Kumar Walia, D. O. Chang and P. Kocher-

lakota, *Phys. Rev. D* **111**, no.10, 104057 (2025).

[29] A. Övgün and M. Fathi, *Nucl. Phys. B* **1018**, 117063 (2025).

[30] D. Pedrotti and M. Calzà, *Phys. Rev. D* **111**, no.12, 12 (2025).

[31] S. Nalui and S. Bhattacharya, *Phys. Lett. B* **861**, 139261 (2025).

[32] P. Hassan Puttasiddappa, D. C. Rodrigues and D. F. Mota, *Eur. Phys. J. C* **85**, no.9, 974 (2025).

[33] R. C. Pantig, S. Kala, A. Övgün and N. J. L. S. Lobos, <https://doi.org/10.1142/S0219887825502408>.

[34] C. Bambi, K. Freese, S. Vagnozzi and L. Visinelli, *Phys. Rev. D* **100**, no.4, 044057 (2019).

[35] K. Jusufi, S. Kumar, M. Azreg-Aïnou, M. Jamil, Q. Wu and C. Bambi, *Eur. Phys. J. C* **82**, no.7, 633 (2022).

[36] J. Solanki and V. Perlick, *Phys. Rev. D* **105**, no.6, 064056 (2022).

[37] A. K. Mishra, S. Chakraborty and S. Sarkar, *Phys. Rev. D* **99**, no.10, 104080 (2019).

[38] R. Ghosh, S. Sk and S. Sarkar, *Phys. Rev. D* **108**, no.4, 4 (2023).

[39] I. Banerjee, S. Chakraborty and S. SenGupta, *Phys. Rev. D* **101**, no.4, 041301 (2020).

[40] I. Banerjee, S. Chakraborty and S. SenGupta, *Phys. Rev. D* **106**, no.8, 084051 (2022).

[41] V. Cardoso, L. C. B. Crispino, C. F. B. Macedo, H. Okawa and P. Pani, *Phys. Rev. D* **90**, no.4, 044069 (2014).

[42] Y. Chen, X. Xue, R. Brito and V. Cardoso, *Phys. Rev. Lett.* **130**, no.11, 111401 (2023).

[43] F. Ozel, D. Psaltis and Z. Younsi, *Astrophys. J.* **941**, no.1, 88 (2022).

[44] C. K. Qiao, P. Su and Y. Huang, *Eur. Phys. J. C* **85**, no.6, 709 (2025).

[45] J. C. Faggert, F. Ozel and D. Psaltis, [arXiv:2506.15783 [astro-ph.HE]].

[46] H. Suzuki, Y. Mizuno, A. Uniyal, I. K. Dihingia, T. Nguyen and C. k. Chan, [arXiv:2511.20756 [astro-ph.HE]].

[47] A. Uniyal, I. K. Dihingia, Y. Mizuno and L. Rezzolla, *Nature Astron.* **1**, 8 (2025).

[48] A. Uniyal, R. C. Pantig and A. Övgün, *Phys. Dark Univ.* **40**, 101178 (2023).

[49] K. Saurabh and K. Jusufi, *Eur. Phys. J. C* **81**, no.6, 490 (2021).

[50] Saurabh *et al.* [Event Horizon Telescope], [arXiv:2512.08970 [astro-ph.HE]].

[51] P. Tiede, M. D. Johnson, D. W. Pesce, D. C. M. Palumbo, D. O. Chang and P. Galison, *Galaxies* **10**, no.6, 111. (2022)

[52] A. E. Broderick, D. W. Pesce, P. Tiede, H. Y. Pu, R. Gold, R. Anantua, S. Britzen, C. Ceccobello, K. Chatterjee and Y. Chen, *et al.* *Astrophys. J.* **935**, 61 (2022).

[53] W. Lockhart and S. E. Gralla, *Mon. Not. Roy. Astron. Soc.* **517**, no.2, 2462-2470 (2022).

[54] S. Paul, *Phys. Rev. D* **102**, no.6, 064045 (2020).

[55] K. S. Virbhadra, *Phys. Rev. D* **106**, no.6, 064038 (2022).

[56] K. S. Virbhadra, *Phys. Rev. D* **79**, 083004 (2009).

[57] K. S. Virbhadra and G. F. R. Ellis, *Phys. Rev. D* **65**, 103004 (2002).

[58] K. S. Virbhadra and G. F. R. Ellis, *Phys. Rev. D* **62**, 084003 (2000).

[59] V. Bozza, *Gen. Rel. Grav.* **42**, 2269-2300 (2010).

[60] D. Chen, Y. Chen, P. Wang, T. Wu and H. Wu, *Eur. Phys. J. C* **84**, no.6, 584 (2024).

[61] M. Khodadi and E. N. Saridakis, *Phys. Dark Univ.* **32**, 100835 (2021).

[62] Saurabh, P. Bambhaniya and P. S. Joshi, <https://arxiv.org/abs/2202.00588>

[63] Y. Chen, R. Roy, S. Vagnozzi and L. Visinelli, *Phys. Rev. D* **106**, no.4, 043021 (2022).

[64] S. Vagnozzi, R. Roy, Y. D. Tsai, L. Visinelli, M. Afrin, A. Allahyari, P. Bambhaniya, D. Dey, S. G. Ghosh and P. S. Joshi, *et al.* *Class. Quant. Grav.* **40**, no.16, 165007 (2023).

[65] M. Khodadi and G. Lambiase, *Phys. Rev. D* **106**, no.10, 104050 (2022).

[66] M. Khodadi, G. Lambiase and D. F. Mota, *JCAP* **09**, 028 (2021).

[67] R. Kumar Walia, *JCAP* **03**, 029 (2023).

[68] F. Eisenhauer *et al.*, *Astrophys. J.* **628**, 246 (2005).

[69] S. Gillessen *et al.*, *Astrophys. J.* **837**, 30 (2017).

[70] M. H. Wu, H. Guo and X. M. Kuang, *Phys. Rev. D* **107**, no.6, 064033 (2023).

[71] X. M. Deng, *Phys. Dark Univ.* **30**, 100629 (2020).

[72] S. Sahu, M. Patil, D. Narasimha, and P. S. Joshi, *Phys. Rev. D* **86**, 063010 – Published 19 September 2012.

[73] S. Sahu, M. Patil, D. Narasimha, and P. S. Joshi, *Phys. Rev. D* **88**, 103002 – Published 6 November 2013.

[74] V. Patel, D. Tahelyani, A. B. Joshi, D. Dey and P. S. Joshi, *Eur. Phys. J. C* **82** (2022) no.9, 798.

[75] N. Tsukamoto, *Phys. Rev. D* **102**, no.10, 104029 (2020).

[76] B. Gao and X. M. Deng, *Annals Phys.* **418**, 168194 (2020).

[77] S. N. Sajadi, M. Khodadi, O. Luongo and H. Quevedo, *Phys. Dark Univ.* **45**, 101525 (2024).

[78] A. B. Joshi, D. Dey, P. S. Joshi and P. Bambhaniya, *Phys. Rev. D* **102**, no.2, 024022 (2020).

[79] A. B. Joshi, K. Mosani and P. S. Joshi, *Phys. Rev. D* **109**, no.6, 064019 (2024).

[80] D. Dey, R. Shaikh and P. S. Joshi, *Phys. Rev. D* **103**,

no.2, 024015 (2021).

[81] K. P. Kaur, P. S. Joshi, D. Dey, A. B. Joshi and R. P. Desai, arXiv:2106.13175 [gr-qc].

[82] M. Khodadi, S. Vagnozzi and J. T. Firouzjaee, *Sci. Rep.* **14**, no.1, 26932 (2024).

[83] D. P. Viththani, A. B. Joshi, T. Bhanja and P. S. Joshi, *Eur. Phys. J. C* **84**, no.4, 383 (2024).

[84] A. Uniyal, I. K. Dihingia, Y. Mizuno and W. Kluźniak, *Astrophys. J.* **993**, no.1, 97 (2025).

[85] D. Tahelyani, A. B. Joshi, D. Dey and P. S. Joshi, arXiv:2205.04055 [gr-qc], (2022).

[86] H. R. Olivares-Sánchez, P. Kocherlakota and C. A. R. Herdeiro, “GRMHD Simulations of Accretion Onto Exotic Compact Objects,” in *New Frontiers in GRMHD Simulations*, edited by Cosimo Bambi, Yosuke Mizuno, Swarnim Shashank, and Feng Yuan *Springer, Singapore*, 2025.

[87] D. Pugliese and Z. Stuchlik, *Eur. Phys. J. C* **84**, no.2, 158 (2024).

[88] S. Patra, B. R. Majhi and S. Das, *JCAP* **01**, 060 (2024).

[89] G. D. Prada-Méndez, F. D. Lora-Clavijo and J. M. Velásquez-Cadavid, *Class. Quant. Grav.* **40**, no.19, 195011 (2023).

[90] D. Pugliese and Z. Stuchlík, *Eur. Phys. J. C* **83**, no.3, 242 (2023). erratum: *Eur. Phys. J. C* **83**, no.4, 303 (2023).

[91] K. Boshkayev, T. Konysbayev, Y. Kurmanov, O. Luongo and D. Malafarina, *Astrophys. J.* **936**, no.2, 96 (2022).

[92] Q. Gan, P. Wang, H. Wu and H. Yang, *Phys. Rev. D* **104**, no.4, 044049 (2021).

[93] Z. Hu, Z. Zhong, P. C. Li, M. Guo and B. Chen, *Phys. Rev. D* **103**, no.4, 044057 (2021).

[94] H. Huang, J. Kunz and D. Mitra, *JCAP* **05**, 007 (2024).

[95] J. C. Feng, S. Chakraborty and V. Cardoso, *Phys. Rev. D* **107**, no.4, 044050 (2023).

[96] F. Di Filippo and L. Rezzolla, *Phys. Rev. D* **111**, no.2, 2 (2025).

[97] C. Bambi and K. Freese, *Phys. Rev. D* **79**, 043002 (2009).

[98] C. Bambi, *Annalen Phys.* **530**, 1700430 (2018).

[99] Ken-ichi Nakao, Chul-Moon Yoo, and Tomohiro Harada *Phys. Rev. D* **99**, 044027 (2019).

[100] Nobuyuki Sakai, Hiromi Saida, and Takashi Tamaki *Phys. Rev. D* **90**, 104013 (2014).

[101] Cosimo Bambi *Phys. Rev. D* **87**, 107501 – Published 3 May 2013.

[102] T. Ohgami and N. Sakai, *Phys. Rev. D* **91**, 124020 (2015).

[103] H. Huang, J. Kunz, J. Yang and C. Zhang, *Phys. Rev. D* **107**, no.10, 104060 (2023).

[104] R. Shaikh, *Mon. Not. Roy. Astron. Soc.* **523**, no.1, 375-384 (2023).

[105] Y. Zhu and T. Wang, *Phys. Rev. D* **104**, no.10, 104052 (2021).

[106] Azreg-Aïnou, M., *Eur. Phys. J. C* **74**, 2865 (2014).

[107] P. V. P. Cunha and C. A. R. Herdeiro, *Phys. Rev. Lett.* **124**, no.18, 181101 (2020).

[108] R. Ghosh and S. Sarkar, *Phys. Rev. D* **104**, no.4, 044019 (2021).

[109] D. N. Solanki, P. Bambhaniya, D. Dey, P. S. Joshi and K. N. Pathak, *Eur. Phys. J. C* **82**, no.1, 77 (2022).

[110] R. Shaikh and P. S. Joshi, *JCAP* **10**, 064 (2019).

[111] J. M. Bardeen, *Non-singular general relativistic gravitational collapse*, in *Proceedings of the International Conference GR5*, Tbilisi, U.S.S.R. (1968).

[112] J. M. Bardeen, [arXiv:1406.4098 [gr-qc]].

[113] T. A. Roman and P. G. Bergmann, *Phys. Rev. D* **28**, 1265-1277 (1983).

[114] V. P. Frolov, *Phys. Rev. D* **94**, no.10, 104056 (2016).

[115] S. A. Hayward, *Phys. Rev. Lett.* **96**, 031103 (2006).

[116] Z. Stuchlik and J. Schee, *Eur. Phys. J. C* **79**, 44 (2019).

[117] P. Bambhaniya, S. K. K. Jusufi and P. S. Joshi, *Phys. Rev. D* **105**, no.2, 023021 (2022).

[118] G. J. Olmo, J. L. Rosa, D. Rubiera-Garcia and D. Saez-Chillon Gomez, *Class. Quant. Grav.* **40**, no.17, 174002 (2023).

[119] K. Boshkayev, T. Konysbayev, Y. Kurmanov, O. Luongo, M. Muccino, A. Taukenova and A. Urazalina, *Eur. Phys. J. C* **84**, no.3, 230 (2024).

[120] R. Kumar and S. G. Ghosh, *Class. Quant. Grav.* **38**, no.8, 8 (2021).

[121] C. Bambi and L. Modesto, *Phys. Lett. B* **721**, 329-334 (2013).

[122] Mustapha Azreg-Aïnou, *Phys. Lett. B* **730**, 95-98 (2014).

[123] K. Pal, K. Pal, R. Shaikh and T. Sarkar, *JCAP* **11**, 060 (2023).

[124] K. Pal, K. Pal, P. Roy and T. Sarkar, *Eur. Phys. J. C* **83**, no.5, 397 (2023).

[125] K. Pal, K. Pal and T. Sarkar, *JCAP* **01**, 069 (2025).

[126] V. P. Frolov, *Nuovo Cim. C* **45**, no.2, 38 (2022).

[127] V. P. Frolov, M. A. Markov and V. F. Mukhanov, *Phys. Rev. D* **41**, 383 (1990).

[128] L. Modesto, *Phys. Rev. D* **70**, 124009 (2004).

[129] A. Ashtekar and M. Bojowald, *Class. Quant. Grav.* **22**, 3349-3362 (2005).

[130] I. Dymnikova, *Gen. Rel. Grav.* **24**, 235-242 (1992).

[131] A. Bonanno and M. Reuter, *Phys. Rev. D* **62**, 043008 (2000).

[132] V. Joshi and A. B. Joshi, [arXiv:2512.07786 [gr-qc]].

[133] M. S. Morris and K. S. Thorne, *Am. J. Phys.* **56**, 395-

412 (1988).

[134] A. Simpson and M. Visser, [JCAP **02**, 042 \(2019\)](#).

[135] E. Franzin, S. Liberati, J. Mazza, A. Simpson and M. Visser, [JCAP **07**, 036 \(2021\)](#).

[136] Y. Guo and Y. G. Miao, [Nucl. Phys. B **983**, 115938 \(2022\)](#).

[137] S. Kala and J. Singh, [Eur. Phys. J. C **85**, no.9, 1047 \(2025\)](#).